

Learning Classical Density Functionals for Ionic Fluids

Anna T. Bui¹ and Stephen J. Cox^{2,*}

¹*Yusuf Hamied Department of Chemistry, University of Cambridge, Lensfield Road, Cambridge, CB2 1EW, United Kingdom*

²*Department of Chemistry, Durham University, South Road, Durham, DH1 3LE, United Kingdom*



(Received 4 October 2024; accepted 4 March 2025; published 11 April 2025)

Accurate and efficient theoretical techniques for describing ionic fluids are highly desirable for many applications across the physical, biological, and materials sciences. With a rigorous statistical mechanical foundation, classical density functional theory (cDFT) is an appealing approach, but the competition between strong Coulombic interactions and steric repulsion limits the accuracy of current approximate functionals. Here, we extend a recently presented machine learning (ML) approach [Sammüller *et al.*, *Proc. Natl. Acad. Sci. U.S.A.*, **120**, e2312484120 (2023)] designed for systems with short-ranged interactions to ionic fluids. By adopting ideas from local molecular field theory, the framework we present amounts to using neural networks to learn the local relationship between the one-body direct correlation functions and inhomogeneous density profiles for a “mimic” short-ranged system, with effects of long-ranged interactions accounted for in a mean-field, yet well-controlled, manner. By comparing to results from molecular simulations, we show that our approach accurately describes the structure and thermodynamics of prototypical models for electrolyte solutions and ionic liquids, including size-asymmetric and multivalent systems. The framework we present acts as an important step toward extending ML approaches for cDFT to systems with accurate interatomic potentials.

DOI: 10.1103/PhysRevLett.134.148001

The behavior of ionic fluids underlies a vast array of physical and biological phenomena as well as technological applications, ranging from electrolyte solutions controlling protein folding [1] to room-temperature ionic liquids in energy storage devices [2]. A fundamental topic that continues to attract enormous interest both experimentally [3–7] and theoretically [8–13] is the structure and thermodynamics of ions near charged interfaces, in particular, how the nature of both the electrolyte and solid surface impacts the properties of the electric double layer (EDL). Poisson–Boltzmann (PB) theory and its linearized Debye–Hückel form provide the basis for much of our understanding of ionic fluids. Their neglect of correlations arising from nonelectrostatic interactions, however, restricts their validity to fluids of low ionic strength.

Classical density functional theory (cDFT) [14–17] provides a natural framework for including correlations omitted by PB theory, and has proven to be a powerful approach to describe equilibrium structure and thermodynamics of fluids in general. While in principle an exact theory, historically, cDFT relies on making approximations

for the excess intrinsic free energy functional $\mathcal{F}_{\text{intr}}^{(\text{ex})}[\{\rho_\nu\}]$, where ρ_ν denotes the one-body density of species ν . For hard sphere fluids, functionals based on Rosenfeld’s fundamental measure theory (FMT) [18–21] have proven highly successful. For simple liquids with square-well, Yukawa, or Lennard–Jones interaction potentials, hard sphere mixtures act as suitable reference systems, with effects of attractive interactions described reasonably well in a mean-field fashion [22–24]. In contrast, existing functionals for ionic fluids are far less accurate, failing to adequately capture the interplay between Coulombic and steric interactions [25–28]. In this Letter, we present a strategy that utilizes machine learning (ML) to construct accurate free energy functionals for ionic fluids.

The rapid advance of modern ML approaches means there has been much recent interest in “learning” representations of the *exact* $\mathcal{F}_{\text{intr}}^{(\text{ex})}[\{\rho_\nu\}]$ [29–35]. Here we build on the method proposed by Sammüller *et al.* [36], in which the one-body direct correlation functions

$$c_\nu^{(1)}(\mathbf{r}; \{\rho_\nu\}) = -\frac{\beta \delta \mathcal{F}_{\text{intr}}^{(\text{ex})}[\{\rho_\nu\}]}{\delta \rho_\nu(\mathbf{r})} \quad (1)$$

are learned by generating inhomogeneous density profiles in the presence of various external and chemical potentials by grand canonical (GC) simulations. This approach to cDFT, dubbed “neural functional theory,” has been shown to outperform FMT-based approaches for both hard sphere

*Contact author: stephen.j.cox@durham.ac.uk

Published by the American Physical Society under the terms of the *Creative Commons Attribution 4.0 International license*. Further distribution of this work must maintain attribution to the author(s) and the published article’s title, journal citation, and DOI.

fluids and Lennard-Jones liquids in terms of both accuracy and speed [36,37].

Two key features underpin the success of the neural functional approach: (i) correlations in the fluid are short-ranged (SR), such that the functional relationship between $c_\nu^{(1)}$ and $\{\rho_\nu\}$ is local; and (ii) the feasibility of GC simulations to produce inhomogeneous density profiles of sufficient quality to form a reliable training set. Ionic fluids pose challenges on both fronts. First, the long-ranged (LR) nature of the Coulomb potential leads to a nonlocal relationship between $c_\nu^{(1)}$ and $\{\rho_\nu\}$. Second, GC simulations for ionic systems raise delicate questions concerning electroneutrality, with various schemes proposed that either insert individual ions or neutral pairs [38–42]. Even then, simulations corresponding exactly to the GC ensemble where the number of each species can fluctuate are impractical, owing to poor acceptance rates of trial insertion and deletion moves. We circumvent both of these issues by adopting concepts from local molecular field theory (LMFT) [43–47], which has been shown to have close links to cDFT [48].

We initially focus our efforts on the prototypical model of an ionic fluid: the restricted primitive model (RPM) comprising oppositely charged hard spheres of equal diameter σ , embedded in a uniform dielectric continuum. Later, we will also present results for a primitive model (i.e., size asymmetric) and a multivalent system. The scheme we propose can be briefly summarized. First, by employing neural networks, we find the one-body direct correlation functions for a suitably chosen “mimic system” whose electrostatic interactions are entirely short ranged. Then, by leveraging LMFT and its relation to cDFT, we account for the net averaged effects of LR electrostatic interactions in a well-controlled fashion. When compared to molecular simulations, the framework we outline describes inhomogeneous density profiles, the equation of state, and the properties of the electric double layer in the presence of electric fields with very high accuracy.

cDFT of a short-ranged “mimic” ionic fluid—Our overall strategy follows that of LMFT, in which we consider a suitably chosen mimic system whose interatomic interactions are entirely short-ranged, and, when subject to a suitably chosen one-body potential ϕ_R , has the same one-body densities as the system of interest with LR interactions (the “full” system). For systems such as the RPM, where LR interactions arise from the Coulomb potential, one adopts the exact splitting

$$1/r = v_0(r) + v_1(r), \quad (2)$$

with $v_0(r) = \text{erfc}(\kappa r)/r$ and $v_1(r) = \text{erf}(\kappa r)/r$. The interatomic potential of the mimic system is then v_0 , and the length scale κ^{-1} is chosen such that the mimic system accurately describes the SR correlations of the full system. In the following, we will work with $\kappa^{-1} = 1.8\sigma$

[see Supplemental Material (SM) [49]]. We will also indicate quantities pertaining to the mimic system with a subscript “R” and focus on behaviors at a reduced temperature $T^* = 0.066$, corresponding to supercritical conditions [67]. The one-body direct correlation functions of the mimic system can be exactly written as

$$c_{R,\nu}^{(1)}(\mathbf{r}) = \ln \Lambda_\nu^3 \rho_{R,\nu}(\mathbf{r}) + \beta V_{R,\nu}(\mathbf{r}) + \beta q_\nu \phi_R(\mathbf{r}) - \beta \mu_{R,\nu}, \quad (3)$$

where Λ_ν , $\mu_{R,\nu}$ and q_ν indicate the thermal de Broglie wavelength, chemical potential, and point charge of species ν , respectively, $V_{R,\nu}$ encompasses any nonelectrostatic contributions to the external potential for species ν , and, for now, ϕ_R is a general external electrostatic potential; we will later discuss how ϕ_R can be chosen such that $\rho_{R,\nu}(\mathbf{r}) = \rho_\nu(\mathbf{r})$.

To learn the functional relationship for $c_{R,\nu}^{(1)}(\mathbf{r}; \{\rho_{R,\nu}\})$, we obtain data for the right hand side of Eq. (3) by measuring $\rho_{R,\nu}$ from simulations with known $\beta V_{R,\nu}$, $\beta \phi_R$, and $\beta \mu_{R,\nu}$. To this end, in line with Ref. [36], we perform GC simulations in a planar geometry at different combinations of $\{\beta V_{R,\nu}\}$, $\beta \phi_R$, and $\{\beta \mu_{R,\nu}\}$. Note that GC simulations are essential for the purpose of evaluating Eq. (3) and, on their own, canonical methods such as molecular dynamics (MD) simulations are insufficient. The form of v_0 means that each particle of the mimic system can be considered electroneutral, comprising both a point charge and a compensating Gaussian charge distribution [68]. As such, in addition to translational moves, we can readily perform GC particle insertions/deletions, along with semi-GC swapping of “anions” and “cations” without needing to worry about issues of electroneutrality [see Fig. 1(a)]. We have found this highly beneficial for converging our simulations, full details of which are provided in SM [49]. In total, ~ 2500 simulations have been performed to gather training data.

For each species, $\nu = +$ or $-$, the neural network used to represent the relationship $\{\rho_{R,\nu}(z)\} \rightarrow c_{R,\nu}^{(1)}(z)$ is structured as follows. The input layer has two channels that are supplied with the discretized values of the cation and anion density profiles in a window $\Delta z = 3.6\sigma$ around the particular value of z . Following a fully connected multi-layer perceptron of three layers, the output layer consists of a single node, which yields the predicted value of $c_{R,\nu}^{(1)}$ at position z . For each ionic fluid considered, we train two independent networks, one for the cation and one for the anion. To reduce noise in the bulk structure predictions, we also obtained models regularized with bulk two-body direct correlation functions as proposed in Ref. [69]. Details of our training procedure are provided in SM [49], and all data are openly available [70].

We first assess the bulk structure predicted by the functional. On the basis of the neural network, we make use of automatic differentiation and radial projection to

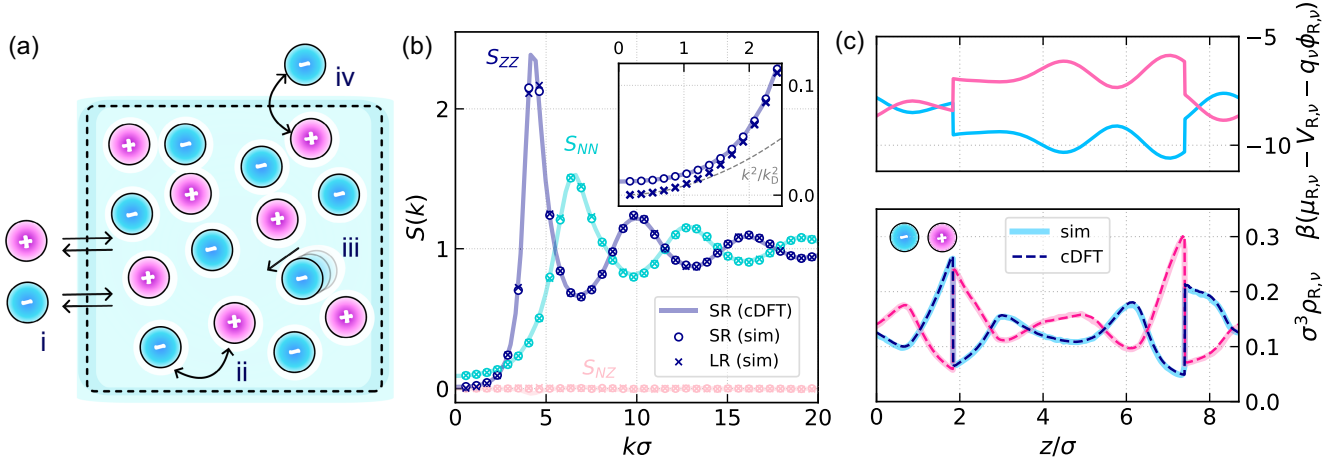


FIG. 1. Structure of the SR mimic RPM. (a) Training data for the neural functional are obtained from GCMC simulations with (i) insertion/deletion, (ii) position swapping, (iii) displacement, and (iv) mutation (identity exchange) moves. (b) The static structure factors from cDFT agree well with results from molecular simulation across the whole range of k for the SR system, shown for a bulk system with $\sigma^3 \rho_{R,\pm} = 0.315$. Inset: At low k , the SR system violates the perfect screening condition, whereas the LR system obeys the Stillinger–Lovett sum rule [see Eq. (5)]. (c) For the applied external potentials (top), predictions of the ion density profiles (bottom) are in excellent agreement with the simulation data.

obtain the partial two-body direct correlation functions $c_{\nu\lambda}^{(2)}(r)$ (see Ref. [36] and SM [49]). By solving the general Ornstein-Zernike equation for mixtures [71,72], we then obtain the total correlation functions $h_{\nu\lambda}^{(2)}(r)$ and the corresponding structure factors $S_{\nu\lambda}(k)$. We further quantify the degree of coupling between number–number (S_{NN}), number–charge (S_{NZ}) and charge–charge (S_{ZZ}) densities by appropriate weighted summations

$$\begin{aligned} S_{NN}(k) &= S_{++}(k) + 2S_{+-}(k) + S_{--}(k), \\ S_{NZ}(k) &= S_{++}(k) - S_{--}(k), \\ S_{ZZ}(k) &= S_{++}(k) - 2S_{+-}(k) + S_{--}(k). \end{aligned} \quad (4)$$

Figure 1(b) shows that the static structure factors obtained from the functional are in excellent agreement with results from a molecular dynamics simulation of the mimic system at the same bulk densities [73]. The symmetry of the RPM is well captured, reflected in $S_{NZ}(k) = 0$. Moreover, by comparing to results from a MD simulation of the full system, we see that $S_{NN}(k)$ and $S_{ZZ}(k)$ for the full and mimic systems agree very well at sufficiently large k , confirming that our choice of $\kappa^{-1} = 1.8\sigma$ is sufficient for the mimic system to capture the SR correlations of the full system. Deviations of the SR system from the LR system only manifest significantly in $S_{ZZ}(k)$ at small k , in agreement with previous works on the subject [46,74]. In particular, as shown in the inset, we see that $S_{ZZ}(k)$ for the LR system strictly obeys the Stillinger-Lovett sum rule [75,76]

$$\lim_{k \rightarrow 0} \frac{k_D^2}{k^2} S_{ZZ}(k) = 1, \quad (5)$$

where k_D^{-1} is the Debye screening length. In contrast, for the mimic system we observe $S_{ZZ}(k) > k^2/k_D^2$ as $k \rightarrow 0$, indicative of a lack of screening. Consistent with the dielectric response of a short-ranged water model [74], these deviations appear at length scales far larger than the range separation prescribed by $2\pi\kappa = 3.5\sigma^{-1}$.

Turning to the ability of cDFT to predict inhomogeneous structure, the equilibrium density profiles of the mimic system can be obtained by self-consistently solving the Euler-Lagrange equation

$$\begin{aligned} \Lambda_\nu^3 \rho_{R,\nu}(\mathbf{r}) &= \exp(-\beta V_{R,\nu}(\mathbf{r}) - \beta q_\nu \phi_R(\mathbf{r}) \\ &\quad + \beta \mu_{R,\nu} + c_{R,\nu}^{(1)}(\mathbf{r}; \{\rho_{R,\nu}\})), \end{aligned} \quad (6)$$

where $c_{R,\nu}^{(1)}$ is evaluated by the corresponding neural network. As shown in Fig. 1(c) for a representative set of external potentials, the resulting $\{\rho_{R,\nu}(z)\}$ from cDFT are in excellent agreement with reference simulation data of the mimic system.

Accounting for long-ranged electrostatics with LMFT—Having established that the cDFT obtained from the ML procedure is accurate for a SR variant of the RPM, we turn our attention to incorporating the effects of LR electrostatic interactions. To do so, we will use concepts from LMFT. The premise of LMFT is that there exists a potential ϕ_R such that

$$\rho_\nu(\mathbf{r}; [\phi], \{\mu_\nu\}) = \rho_{R,\nu}(\mathbf{r}; [\phi_R], \{\mu_{R,\nu}\}). \quad (7)$$

In Eq. (7), we have explicitly indicated the functional dependence of the densities on the external electrostatic potential [77]. As shown in Ref. [48], when recast in a

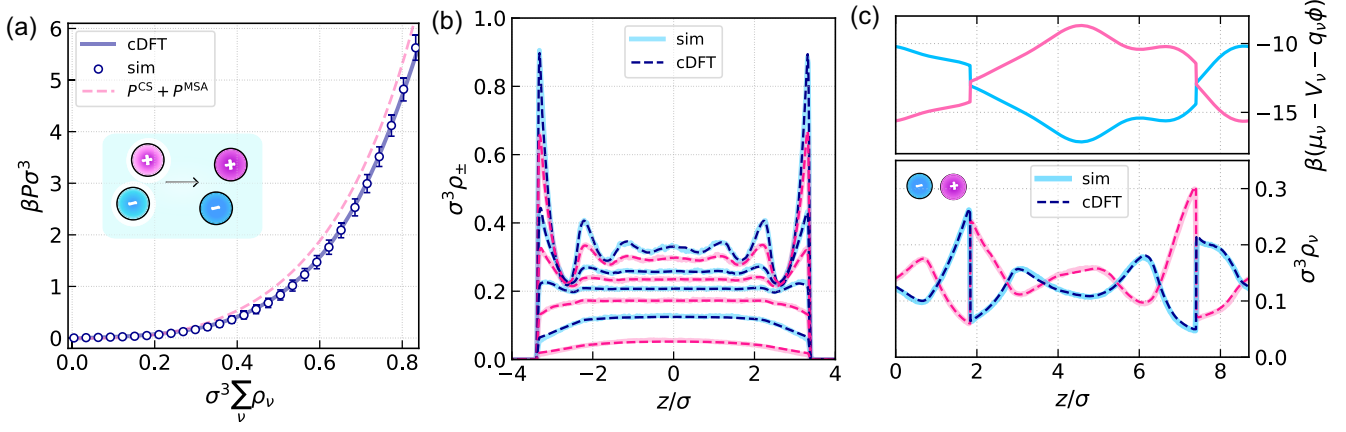


FIG. 2. Structure and thermodynamics of the LR full system. cDFT for the RPM at $T^* = 0.066$ with effects of LR electrostatic interactions accounted by LMFT shows excellent agreement with reference molecular simulation data for (a) the equation of state, (b) ion density profiles confined in a slit, and (c) with an applied external potential. In (a), we see that our cDFT approach outperforms the prediction obtained by combining the Carnahan-Starling equation of state for hard-sphere fluids (P^{CS}) and the mean spherical approximation (P^{MSA}). For the LR system in (c), the applied external potential acts over a much longer range and the chemical potentials are shifted lower compared to the SR mimic system in Fig. 1(c) to yield $\rho_{\nu}(z) = \rho_{R,\nu}(z)$.

cDFT framework, LMFT relates the one-body direct correlation functions of the full and mimic systems through

$$c_{\nu}^{(1)}(\mathbf{r}; [\{\rho_{\nu}\}]) = c_{R,\nu}^{(1)}(\mathbf{r}; [\{\rho_{\nu}\}]) - \beta \Delta \mu_{\nu} + \beta q_{\nu} \Delta \phi(\mathbf{r}), \quad (8)$$

which is an exact result. A key insight from LMFT [43,44] is that for an appropriate splitting of the potential [see Eq. (2)], $\Delta \phi$ is well-approximated by a mean field form

$$\Delta \phi(\mathbf{r}) \equiv \phi(\mathbf{r}) - \phi_R(\mathbf{r}) = -\frac{1}{\epsilon} \int d\mathbf{r}' n(\mathbf{r}') v_1(|\mathbf{r} - \mathbf{r}'|), \quad (9)$$

where ϵ is the dielectric constant of the continuum and $n = n_R = \sum_{\nu} q_{\nu} \rho_{\nu}$ is the charge density. For homogeneous systems, Rodgers and Weeks have also derived a thermodynamic correction for the total energy, from which a correction for the pressure follows [78],

$$\Delta P \equiv P - P_R = -\frac{k_B T}{2\pi^{3/2} \kappa^{-3}}. \quad (10)$$

Based on Ref. [78], we have further derived a correction for the chemical potential (see SM [49]),

$$\Delta \mu_{\nu} \equiv \mu_{\nu} - \mu_{R,\nu} = -\frac{q_{\nu}^2}{\kappa^{-1} \sqrt{\pi}}. \quad (11)$$

We first consider the bulk thermodynamics of the RPM. The equation of state for the LR system is obtained with

$$P(\{\rho_{\nu}\}) = \sum_{\nu} k_B T \rho_{\nu} (1 - c_{R,\nu}^{(1)}[\{\rho_{\nu}\}]) - \frac{\mathcal{F}_{\text{intr},R}^{(\text{ex})}[\{\rho_{\nu}\}]}{V} + \Delta P, \quad (12)$$

where the sum of the first two terms is the negative of the grand potential density of the mimic system. The excess free

energy $\mathcal{F}_{\text{intr},R}^{(\text{ex})}$ is accessible by functional line integration. The result of this procedure, shown in Fig. 2(a), agrees very well with reference simulation data. We also see that, particularly at higher densities, Eq. (12) performs significantly better than the analytical approximation that results from adding the Carnahan-Starling equation of state (P^{CS}) [79] and the mean spherical approximation (P^{MSA}) [80,81], despite the fact that $P^{CS} + P^{MSA}$ forms the basis for the vast majority of current state-of-the-art functionals for ionic fluids [27,28].

The advantages of cDFT combined with LMFT become even clearer when inhomogeneous systems are considered. The equilibrium densities of the full system are given by

$$\Lambda_{\nu}^3 \rho_{\nu}(\mathbf{r}) = \exp(-\beta V_{\nu}(\mathbf{r}) - \beta q_{\nu} \phi(\mathbf{r}) + \beta \mu_{\nu} + c_{\nu}^{(1)}(\mathbf{r}; [\{\rho_{\nu}\}])), \quad (13)$$

where the nonlocal functional $c_{\nu}^{(1)}$ is now given by Eq. (8), together with Eqs. (9) and (11). From a cDFT perspective, we have captured all strong rapidly varying short-ranged correlations with the neural networks for $c_{R,\nu}^{(1)}$, while the effects of LR electrostatic interactions are incorporated in a mean-field yet well-controlled fashion.

In practical terms, for a planar geometry, Eq. (9) can be recast as

$$\Delta \phi(z) = -\frac{1}{\epsilon L} \sum_{k \neq 0} \frac{4\pi}{k^2} \tilde{n}(k) \exp(ikz) \exp\left(-\frac{k^2}{4\kappa^2}\right), \quad (14)$$

where \tilde{n} denotes a Fourier component of n , and L is the total length of the periodic cell. In Fig. 2(b), we show the results from our cDFT approach for the RPM confined between two repulsive walls for various values of $\mu_{+} = \mu_{-}$. The density

profiles are in very good agreement with reference canonical MD simulation data in which the number of particles matches that obtained by integrating the density profiles from cDFT. Our cDFT approach also works very well in cases where the external potential contains an electrostatic component, as illustrated in Fig. 2(c). Here, the full system is the LR counterpart of the mimic system shown in Fig. 1(c), emphasizing the premise of LMFT [see Eq. (7)].

The electric double layer and other ionic fluids—The results presented so far demonstrate that our cDFT approach provides an efficient and accurate route to the structure and thermodynamics of the RPM. As an application, we turn our attention to the fundamental topic of ongoing scientific interest: the electric double layer. We also show that our approach is robust to the choice of interatomic potential. Specifically, we also consider the primitive model (PM) and a multivalent fluid.

As a simple model of an EDL-forming system, we consider the RPM confined between two repulsive walls, and in the presence of an electric field E_z along the z direction. The electrostatic potential that the LR system feels is $\phi(z) = -E_z z$. For the reference simulation data, the LR system was simulated at constant E_z using the finite-field approach [82–88]. As shown in Fig. 3(a), the ion distributions from our cDFT approach are in excellent agreement with the results from simulations. Notably, the cDFT accurately describes the strong oscillations in the density profiles of co- and counterions. Moreover, as we detail in SM [49], our functional is thermodynamically consistent, satisfying the contact density theorem [89–91]

$$P = -\sum_{\nu} \int dz \rho_{\nu}(z) \frac{dV_{\nu}(z)}{dz} - \frac{2\pi\sigma_s^2}{\epsilon}, \quad (15)$$

which relates the bulk pressure to the surface charge density $\sigma_s = \int_{-L}^0 dz n(z)$ [92] and ion densities at contact with the walls. Obeying this contact theorem has proven a challenge not only for integral equation methods [93–96], which tend to violate key sum rules and are therefore generally thermodynamically inconsistent [48,97], but also for most state-of-the-art cDFT functionals for ionic fluids [98,99]. The accurate description of EDL structure and thermodynamic consistency displayed by our LMFT-based neural cDFT approach constitutes a significant advancement in the theoretical description of ionic fluids.

The main advantage of the neural functional approach outlined in Ref. [36] is arguably that the local relationship between $c_{\nu}^{(1)}$ and $\{\rho_{\nu}\}$ permits application of the resulting functional to system sizes far beyond those encountered during training of the ML. By using the framework of LMFT and its relationship to cDFT, we have successfully extended the neural functional approach to a case where the relationship between $c_{\nu}^{(1)}$ and $\{\rho_{\nu}\}$ is nonlocal. To demonstrate that this methodology is not limited to the RPM, in Figs. 3(b) and 3(c), we present results for a PM and multivalent system. For the PM, we have changed the sizes of the anion and

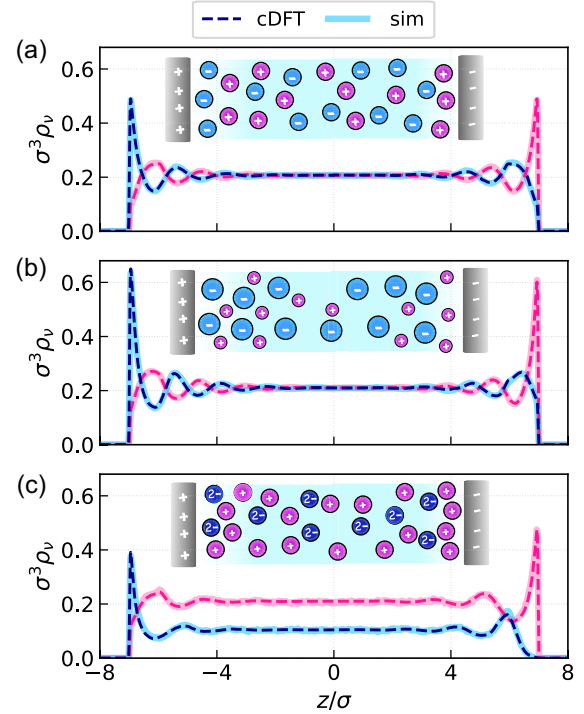


FIG. 3. Accurately describing the EDL with cDFT for (a) the RPM, (b) the PM, and (c) a multivalent fluid. In all cases, confining walls are located at $z/\sigma = \pm 7.2$ in a periodic cell of $L/\sigma = 18.1$, and $E_z = 1.7k_B T/e\sigma$. The resulting ion density profiles from cDFT are in excellent agreement with molecular simulations, and obey the contact theorem [Eq. (15)].

cation to $\sigma_- = 4\sigma/3$ and $\sigma_+ = 2\sigma/3$, respectively. For the multivalent system, we consider equal-sized anions and cations of diameter σ , but increase the valency of the anion such that $q_-/q_+ = 2$. We use the same temperature as for the RPM, $T^* = \epsilon\sigma k_B T/|q_+ q_-| = 0.066$. In both cases, we observe excellent agreement between the neural cDFT and simulations, both for inhomogeneous profiles and bulk equations of state, as further shown in SM [49]. Future work will pursue using neural functionals to understand EDL capacitance [100] and surface force balance measurements [13], and to augment other cDFT approaches to understand solvation [101]. The framework we have outlined should also find use in describing the dielectric response of polar fluids such as water [74,102,103].

Acknowledgments—Via membership of the UK’s HEC Materials Chemistry Consortium funded by EPSRC (EP/X035859), this work used the ARCHER2 UK National Supercomputing Service. A.T.B. acknowledges funding from the Oppenheimer Fund and Peterhouse College, University of Cambridge. S.J.C. is a Royal Society University Research Fellow (Grant No. URF\R1\211144) at Durham University.

Data availability—Training data and code supporting the findings of this study will be openly available [66,70].

- [1] W. Kunz, J. Henle, and B. W. Ninham, ‘Zur Lehre von der Wirkung der Salze’ (about the science of the effect of salts): Franz Hofmeister’s historical papers, *Curr. Opin. Colloid Interface Sci.* **9**, 19 (2004).
- [2] S. Kondrat, G. Feng, F. Bresme, M. Urbakh, and A. A. Kornyshev, Theory and simulations of ionic liquids in nanoconfinement, *Chem. Rev.* **123**, 6668 (2023).
- [3] R. M. Espinosa-Marzal, A. Arcifa, A. Rossi, and N. D. Spencer, Microslips to “avalanches” in confined, molecular layers of ionic liquids, *J. Phys. Chem. Lett.* **5**, 179 (2014).
- [4] M. A. Gebbie, H. A. Dobbs, M. Valtiner, and J. N. Israelachvili, Long-range electrostatic screening in ionic liquids, *Proc. Natl. Acad. Sci. U.S.A.* **112**, 7432 (2015).
- [5] A. M. Smith, A. A. Lee, and S. Perkin, The electrostatic screening length in concentrated electrolytes increases with concentration, *J. Phys. Chem. Lett.* **7**, 2157 (2016).
- [6] A. A. Lee, C. S. Perez-Martinez, A. M. Smith, and S. Perkin, Underscreening in concentrated electrolytes, *Faraday Discuss.* **199**, 239 (2017).
- [7] M. A. Gebbie, A. M. Smith, H. A. Dobbs, A. A. Lee, G. G. Warr, X. Banquy, M. Valtiner, M. W. Rutland, J. N. Israelachvili, S. Perkin, and R. Atkin, Long range electrostatic forces in ionic liquids, *Chem. Commun. (Cambridge)* **53**, 1214 (2017).
- [8] G. M. Torrie and J. P. Valleau, Electrical double layers. I. Monte Carlo study of a uniformly charged surface, *J. Chem. Phys.* **73**, 5807 (1980).
- [9] C. Merlet, D. T. Limmer, M. Salanne, R. van Roij, P. A. Madden, D. Chandler, and B. Rotenberg, The electric double layer has a life of its own, *J. Phys. Chem. C* **118**, 18291 (2014).
- [10] M. Z. Bazant, B. D. Storey, and A. A. Kornyshev, Double layer in ionic liquids: Overscreening versus crowding, *Phys. Rev. Lett.* **106**, 046102 (2011).
- [11] F. Coupette, A. A. Lee, and A. Härtel, Screening lengths in ionic fluids, *Phys. Rev. Lett.* **121**, 075501 (2018).
- [12] J. P. de Souza, Z. A. H. Goodwin, M. McEldrew, A. A. Kornyshev, and M. Z. Bazant, Interfacial layering in the electric double layer of ionic liquids, *Phys. Rev. Lett.* **125**, 116001 (2020).
- [13] P. Cats, R. Evans, A. Härtel, and R. van Roij, Primitive model electrolytes in the near and far field: Decay lengths from DFT and simulations, *J. Chem. Phys.* **154**, 124504 (2021).
- [14] R. Evans, The nature of the liquid-vapour interface and other topics in the statistical mechanics of non-uniform, classical fluids, *Adv. Phys.* **28**, 143 (1979).
- [15] R. Evans, *Fundamentals of Inhomogeneous Fluids*, edited by D. Henderson (Dekker, New York, 1992).
- [16] J. F. Lutsko, Recent Developments in Classical Density Functional Theory, *Adv. Chem. Phys.* (John Wiley & Sons, New York, 2010) pp. 1–92, [10.1002/9780470564318.ch1](https://doi.org/10.1002/9780470564318.ch1).
- [17] J. Hansen and I. McDonald, *Theory of Simple Liquids: With Applications to Soft Matter* (Elsevier Science, New York, 2013).
- [18] Y. Rosenfeld, Free-energy model for the inhomogeneous hard-sphere fluid mixture and density-functional theory of freezing, *Phys. Rev. Lett.* **63**, 980 (1989).
- [19] R. Roth, R. Evans, A. Lang, and G. Kahl, Fundamental measure theory for hard-sphere mixtures revisited: The White Bear version, *J. Phys. Condens. Matter* **14**, 12063 (2002).
- [20] H. Hansen-Goos and R. Roth, Density functional theory for hard-sphere mixtures: The White Bear version mark II, *J. Phys. Condens. Matter* **18**, 8413 (2006).
- [21] R. Roth, Fundamental measure theory for hard-sphere mixtures: A review, *J. Phys. Condens. Matter* **22**, 063102 (2010).
- [22] E. Kierlik and M. L. Rosinberg, Density-functional theory for inhomogeneous fluids: Adsorption of binary mixtures, *Phys. Rev. A* **44**, 5025 (1991).
- [23] M. C. Stewart and R. Evans, Wetting and drying at a curved substrate: Long-ranged forces, *Phys. Rev. E* **71**, 011602 (2005).
- [24] A. J. Archer, B. Chacko, and R. Evans, The standard mean-field treatment of inter-particle attraction in classical DFT is better than one might expect, *J. Chem. Phys.* **147**, 034501 (2017).
- [25] A. Härtel, M. Janssen, S. Samin, and R. v. Roij, Fundamental measure theory for the electric double layer: Implications for blue-energy harvesting and water desalination, *J. Phys. Condens. Matter* **27**, 194129 (2015).
- [26] A. Härtel, Structure of electric double layers in capacitive systems and to what extent (classical) density functional theory describes it, *J. Phys. Condens. Matter* **29**, 423002 (2017).
- [27] R. Roth and D. Gillespie, Shells of charge: A density functional theory for charged hard spheres, *J. Phys. Condens. Matter* **28**, 244006 (2016).
- [28] M. Bültmann and A. Härtel, The primitive model in classical density functional theory: Beyond the standard mean-field approximation, *J. Phys. Condens. Matter* **34**, 235101 (2022).
- [29] P. Cats, S. Kuipers, S. de Wind, R. van Damme, G. M. Coli, M. Dijkstra, and R. van Roij, Machine-learning free-energy functionals using density profiles from simulations, *APL Mater.* **9**, 031109 (2021).
- [30] J. Dijkman, M. Dijkstra, R. van Roij, M. Welling, J.-W. van de Meent, and B. Ensing, Learning neural free-energy functionals with pair-correlation matching, *Phys. Rev. Lett.* **134**, 056103 (2025).
- [31] A. Simon and M. Oettel, Machine learning approaches to classical density functional theory, [arXiv:2406.07345](https://arxiv.org/abs/2406.07345).
- [32] S.-C. Lin, G. Martius, and M. Oettel, Analytical classical density functionals from an equation learning network, *J. Chem. Phys.* **152**, 021102 (2020).
- [33] L. Shang-Chun and M. Oettel, A classical density functional from machine learning and a convolutional neural network, *SciPost Phys.* **6**, 025 (2019).
- [34] A. Malpica-Morales, P. Yatsyshin, M. A. Durán-Olivencia, and S. Kalliadasis, Physics-informed Bayesian inference of external potentials in classical density-functional theory, *J. Chem. Phys.* **159**, 104109 (2023).
- [35] R. Pederson, B. Kalita, and K. Burke, Machine learning and density functional theory, *Nat. Rev. Phys.* **4**, 357 (2022).

- [36] F. Sammüller, S. Hermann, D. de las Heras, and M. Schmidt, Neural functional theory for inhomogeneous fluids: Fundamentals and applications, *Proc. Natl. Acad. Sci. U.S.A.* **120**, e2312484120 (2023).
- [37] F. Sammüller, M. Schmidt, and R. Evans, Neural density functional theory of liquid-gas phase coexistence, *Phys. Rev. X* **15**, 011013 (2025).
- [38] J.C. Shelley and G.N. Patey, A configuration bias Monte Carlo method for ionic solutions, *J. Chem. Phys.* **100**, 8265 (1994).
- [39] Q. Yan and J.J. de Pablo, Hyper-parallel tempering Monte Carlo: Application to the Lennard-Jones fluid and the restricted primitive model, *J. Chem. Phys.* **111**, 9509 (1999).
- [40] F. Moučka, M. Lísal, J. Škvor, J. Jirsák, I. Nezbeda, and W.R. Smith, Molecular simulation of aqueous electrolyte solubility. 2. Osmotic ensemble Monte Carlo methodology for free energy and solubility calculations and application to NaCl, *J. Phys. Chem. B* **115**, 7849 (2011).
- [41] F. Moučka, D. Bratko, and A. Luzar, Electrolyte pore/solution partitioning by expanded grand canonical ensemble Monte Carlo simulation, *J. Chem. Phys.* **142**, 124705 (2015).
- [42] J. Kim, L. Belloni, and B. Rotenberg, Grand-canonical molecular dynamics simulations powered by a hybrid 4D nonequilibrium MD/MC method: Implementation in LAMMPS and applications to electrolyte solutions, *J. Chem. Phys.* **159**, 144802 (2023).
- [43] J.M. Rodgers and J.D. Weeks, Local molecular field theory for the treatment of electrostatics, *J. Phys. Condens. Matter* **20**, 494206 (2008).
- [44] J.D. Weeks, K. Katsov, and K. Vollmayr, Roles of repulsive and attractive forces in determining the structure of nonuniform liquids: Generalized mean field theory, *Phys. Rev. Lett.* **81**, 4400 (1998).
- [45] J.M. Rodgers, C. Kaur, Y.-G. Chen, and J.D. Weeks, Attraction between like-charged walls: Short-ranged simulations using local molecular field theory, *Phys. Rev. Lett.* **97**, 097801 (2006).
- [46] Y.-g. Chen, C. Kaur, and J.D. Weeks, Connecting systems with short and long ranged interactions: Local molecular field theory for ionic fluids, *J. Phys. Chem. B* **108**, 19874 (2004).
- [47] R.C. Remsing, S. Liu, and J.D. Weeks, Long-ranged contributions to solvation free energies from theory and short-ranged models, *Proc. Natl. Acad. Sci. U.S.A.* **113**, 2819 (2016).
- [48] A.J. Archer and R. Evans, Relationship between local molecular field theory and density functional theory for non-uniform liquids, *J. Chem. Phys.* **138**, 014502 (2013).
- [49] See Supplemental Material at <http://link.aps.org/supplemental/10.1103/PhysRevLett.134.148001>, which includes Refs. [50–66], for additional information on simulation details, training procedure, derivation of $\Delta\mu_\nu$, and additional results.
- [50] A.Z. Panagiotopoulos, *Molecular simulation of phase equilibria: Simple, ionic and polymeric fluids, *Fluid Phase Equilib.* **76**, 97 (1992).
- [51] A.P. Thompson, H.M. Aktulga, R. Berger, D.S. Bolintineanu, W.M. Brown, P.S. Crozier, P.J. in 't Veld, A. Kohlmeyer, S.G. Moore, T.D. Nguyen, R. Shan, M.J. Stevens, J. Tranchida, C. Trott, and S.J. Plimpton, LAMMPS—a flexible simulation tool for particle-based materials modeling at the atomic, meso, and continuum scales, *Comput. Phys. Commun.* **271**, 108171 (2022).
- [52] T. Schneider and E. Stoll, Molecular-dynamics study of a three-dimensional one-component model for distortive phase transitions, *Phys. Rev. B* **17**, 1302 (1978).
- [53] A. Härtel, S. Samin, and R. van Roij, Dense ionic fluids confined in planar capacitors: In- and out-of-plane structure from classical density functional theory, *J. Phys. Condens. Matter* **28**, 244007 (2016).
- [54] J. Jover, A.J. Haslam, A. Galindo, G. Jackson, and E.A. Müller, Pseudo hard-sphere potential for use in continuous molecular-dynamics simulation of spherical and chain molecules, *J. Chem. Phys.* **137**, 144505 (2012).
- [55] A.V. Brukhno, J. Grant, T.L. Underwood, K. Stratford, S.C. Parker, J.A. Purton, and N.B. Wilding, DL_MONTE: A multipurpose code for Monte Carlo simulation, *Mol. Simul.* **47**, 131 (2021).
- [56] S.W. de Leeuw, J.W. Perram, E.R. Smith, and J.S. Rowlinson, Simulation of electrostatic systems in periodic boundary conditions. I. Lattice sums and dielectric constants, *Proc. R. Soc. A* **373**, 27 (1997).
- [57] R. Hockney and J. Eastwood, *Computer Simulation Using Particles* (Adam-Hilger, New York, 1988).
- [58] J. Kolafa and J.W. Perram, Cutoff errors in the Ewald summation formulae for point charge systems, *Mol. Simul.* **9**, 351 (1992).
- [59] F. Chollet, *Deep Learning with Python* (Manning Publications, New York, 2017), <https://www.manning.com/books/deep-learning-with-python>.
- [60] T. Sayer, C. Zhang, and M. Sprik, Charge compensation at the interface between the polar NaCl(111) surface and a NaCl aqueous solution, *J. Chem. Phys.* **147**, 104702 (2017).
- [61] T. Sayer, M. Sprik, and C. Zhang, Finite electric displacement simulations of polar ionic solid-electrolyte interfaces: application to NaCl(111)/aqueous NaCl solution, *J. Chem. Phys.* **150**, 041716 (2019).
- [62] F. Sedlmeier, D. Horinek, and R.R. Netz, Spatial correlations of density and structural fluctuations in liquid water: A comparative simulation study, *J. Am. Chem. Soc.* **133**, 1391 (2011).
- [63] J.K. Johnson, J.A. Zollweg, and K.E. Gubbins, The Lennard-Jones equation of state revisited, *Mol. Phys.* **78**, 591 (1993).
- [64] A.T. Bui, GCMC with Gaussian truncated potentials, <https://github.com/annatbui/GCMC> (2024).
- [65] S.J. Cox, Gaussian truncated potentials in LAMMPS, <https://github.com/uccasco/LMFT> (2020).
- [66] A.T. Bui and S.J. Cox, Learning cDFT for ionic fluids, <https://github.com/annatbui/ion-cdft> (2024).
- [67] The critical temperature of the RPM is $T_c^* = 0.0492$ (from Ref. [39]).
- [68] D. Frenkel and B. Smit, *Understanding Molecular Simulation: From Algorithms to Applications* (Elsevier Science, New York, 2023).

- [69] F. Sammüller and M. Schmidt, Neural density functionals: Local learning and pair-correlation matching, *Phys. Rev. E* **110**, L032601 (2024).
- [70] A. T. Bui and S. J. Cox, Research data supporting “Learning classical density functionals for ionic fluids”, Zenodo (2024), [10.5281/zenodo.15085645](https://doi.org/10.5281/zenodo.15085645).
- [71] L. S. Ornstein and F. Zernike, Accidental deviations of density and opalescence at the critical point of a single substance, *Proc. R. Neth. Acad. Arts Sci.* **17**, 793 (1914).
- [72] R. J. Baxter, Ornstein–Zernike relation and Percus–Yevick approximation for fluid mixtures, *J. Chem. Phys.* **52**, 4559 (2003).
- [73] While GC simulations (i.e., known $\{\mu_\nu\}$) are required to train the neural networks [see Eq. (3)], it is reasonable to compare to average structures obtained with canonical simulations at the same average density.
- [74] S. J. Cox, Dielectric response with short-ranged electrostatics, *Proc. Natl. Acad. Sci. U.S.A.* **117**, 19746 (2020).
- [75] F. H. Stillinger and R. Lovett, General restriction on the distribution of ions in electrolytes, *J. Chem. Phys.* **49**, 1991 (1968).
- [76] F. H. Stillinger and R. Lovett, Ion-pair theory of concentrated electrolytes. I. Basic concepts, *J. Chem. Phys.* **48**, 3858 (1968).
- [77] The number densities also have a functional dependence on the non-electrostatic contribution to the external potential. As this is the same for both the full and mimic systems, i.e. $\{V_\nu\} = \{V_{\nu,R}\}$, we do not indicate this functional dependence explicitly in Eq. (7).
- [78] J. M. Rodgers and J. D. Weeks, Accurate thermodynamics for short-ranged truncations of Coulomb interactions in site-site molecular models, *J. Chem. Phys.* **131**, 244108 (2009).
- [79] N. F. Carnahan and K. E. Starling, Equation of state for nonattracting rigid spheres, *J. Chem. Phys.* **51**, 635 (1969).
- [80] J. L. Lebowitz and J. K. Percus, Mean spherical model for lattice gases with extended hard cores and continuum fluids, *Phys. Rev.* **144**, 251 (1966).
- [81] L. Blum, Mean spherical model for asymmetric electrolytes, *Mol. Phys.* **30**, 1529 (1975).
- [82] M. Stengel, N. A. Spaldin, and D. Vanderbilt, Electric displacement as the fundamental variable in electronic-structure calculations, *Nat. Phys.* **5**, 304 (2009).
- [83] C. Zhang and M. Sprik, Computing the dielectric constant of liquid water at constant dielectric displacement, *Phys. Rev. B* **93**, 144201 (2016).
- [84] C. Zhang and M. Sprik, Finite field methods for the supercell modeling of charged insulator/electrolyte interfaces, *Phys. Rev. B* **94**, 245309 (2016).
- [85] M. Sprik, Finite Maxwell field and electric displacement Hamiltonians derived from a current dependent Lagrangian, *Mol. Phys.* **116**, 3114 (2018).
- [86] S. J. Cox and M. Sprik, Finite field formalism for bulk electrolyte solutions, *J. Chem. Phys.* **151**, 064506 (2019).
- [87] T. Sayer and S. J. Cox, Macroscopic surface charges from microscopic simulations, *J. Chem. Phys.* **153**, 164709 (2020).
- [88] C. Zhang, T. Sayer, J. Hutter, and M. Sprik, Modelling electrochemical systems with finite field molecular dynamics, *J. Phys. Energy* **2**, 032005 (2020).
- [89] D. Henderson and L. Blum, Some exact results and the application of the mean spherical approximation to charged hard spheres near a charged hard wall, *J. Chem. Phys.* **69**, 5441 (1978).
- [90] D. Henderson, L. Blum, and J. L. Lebowitz, An exact formula for the contact value of the density profile of a system of charged hard spheres near a charged wall, *J. Electroanal. Chem.* **102**, 315 (1979).
- [91] P. A. Martin, Sum rules in charged fluids, *Rev. Mod. Phys.* **60**, 1075 (1988).
- [92] This equation for σ_s assumes that the electrolyte is centered in a periodically replicated cell of length L along the z direction.
- [93] T. Ichiye and A. D. J. Haymet, Integral equation theory of ionic solutions, *J. Chem. Phys.* **93**, 8954 (1990).
- [94] K. Nygård, S. Sarman, and R. Kjellander, Local order variations in confined hard-sphere fluids, *J. Chem. Phys.* **139**, 164701 (2013).
- [95] Y. Jing, V. Jadhao, J. W. Zwanikken, and M. Olvera de la Cruz, Ionic structure in liquids confined by dielectric interfaces, *J. Chem. Phys.* **143**, 194508 (2015).
- [96] M. Dinpajoo, N. N. Intan, T. T. Duignan, E. Biasin, J. L. Fulton, S. M. Kathmann, G. K. Schenter, and C. J. Mundy, Beyond the Debye–Hückel limit: Toward a general theory for concentrated electrolytes, *J. Chem. Phys.* **161**, 230901 (2024).
- [97] J. R. Henderson, *Fundamentals of Inhomogeneous Fluids*, edited by D. Henderson (Dekker, New York, 1992).
- [98] A. Voukadinova, M. Valiskó, and D. Gillespie, Assessing the accuracy of three classical density functional theories of the electrical double layer, *Phys. Rev. E* **98**, 012116 (2018).
- [99] D. Gillespie, Restoring the consistency with the contact density theorem of a classical density functional theory of ions at a planar electrical double layer, *Phys. Rev. E* **90**, 052134 (2014).
- [100] P. Cats and R. van Roij, The differential capacitance as a probe for the electric double layer structure and the electrolyte bulk composition, *J. Chem. Phys.* **155**, 104702 (2021).
- [101] A. T. Bui and S. J. Cox, A classical density functional theory for solvation across length scales, *J. Chem. Phys.* **161**, 104103 (2024).
- [102] A. Gao, R. C. Remsing, and J. D. Weeks, Local molecular field theory for Coulomb interactions in aqueous solutions, *J. Phys. Chem. B* **127**, 809 (2023).
- [103] J. M. Rodgers and J. D. Weeks, Interplay of local hydrogen-bonding and long-ranged dipolar forces in simulations of confined water, *Proc. Natl. Acad. Sci. U.S.A.* **105**, 19136 (2008).